Quantitative Assessment of Condylar Bone Changes in Osteoarthritis Patients Using Single-photon emission computed tomography/computed tomography and Magnetic resonance imaging

Lee, Chaeyeon

Department of Dentistry

Graduate School

Yonsei University

Quantitative Assessment of Condylar Bone Changes in Osteoarthritis Patients Using Single-photon emission computed tomography/computed tomography and Magnetic resonance imaging

Advisor Kim, Jae-Young

A Master's Thesis Submitted

to the Department of Dentistry

and the Committee on Graduate School

of Yonsei University in Partial Fulfillment of the

Requirements for the Degree of

Master of Dental Science

Lee, Chaeyeon

June 2025

Quantitative Assessment of Condylar Bone Changes in Osteoarthritis Patients Using Single-photon emission computed tomography/computed tomography and Magnetic resonance imaging

This Certifies that the Master's Thesis of Chaeyeon Lee is Approved

`

Committee Chair	**Huh, Jong-Ki**
Committee Member	**Kim, Jae-Young**
Committee Member	**Jeon, Kug Jin**

Department of Dentistry
Graduate School
Yonsei University
June 2025

감사의 글

석사과정을 마무리하며, 이 자리를 빌려 제 곁에서 아낌없는 사랑과 격려를 보내주신 모든 분들께 진심으로 감사의 말씀을 전하고자 합니다.

무엇보다도 언제나 저를 믿어주시고 늘 지원해주신 부모님께 큰 감사를 드립니다. 사랑과 헌신으로 지금의 제가 있기까지 늘 든든한 버팀목이 되어주셨습니다. 연구자로서의 첫걸음을 내딛는 데 있어, 제게 연구의 본질과 자세를 가르쳐주신 김재영 교수님께 진심으로 감사드립니다. 교수님의 세심한 지도를 통해 학문적 성장뿐 아니라 연구자로서의 태도를 배울 수 있었습니다. 수련 기간 동안 따뜻한 관심과 사랑으로 성장할 수 있도록 이끌어주신 허종기 교수님과 김혜선 교수님께도 깊은 감사의 말씀을 드립니다. 또한, 논문 심사위원으로 참여해주시며 부족한 부분을 꼼꼼히 짚어주시고 방향을 제시해주신 전국진 교수님께도 감사드립니다. 마지막으로, 임상강사로서 새롭게 시작하는 여정에서, 더 성장할 수 있도록 지도해주시는 정영수 교수님, 박진후 교수님, 김준영 교수님, 조현미 교수님께도 감사의 마음을 전합니다.

2025년 7월

이 채 연

TABLE OF CONTENTS

LIST OF FIGURES

LIST OF TABLES

ABSTRACT

Quantitative Assessment of Condylar Bone Changes in Osteoarthritis Patients Using Single-photon emission computed tomography/computed tomography and Magnetic resonance imaging

Temporomandibular joint osteoarthritis (TMJ OA) is a chronic condition characterized by degenerative changes in the articular cartilage, accompanied with bony remodeling and functional deterioration. Clinically, it leads to pain during mastication, limited mouth opening, and joint sounds. However, these symptoms are subjective and may arise from various causes; therefore, imaging evaluation is essential for accurate diagnosis.

Whereas conventional radiographs only allow for the evaluation of morphological changes in bone, recent advances in functional imaging techniques have enabled quantitative analysis reflecting bone metabolism and vascular status. Accordingly, this study aimed to comprehensively evaluate condylar bone metabolism, density, and blood perfusion status in TMJ OA patients using the maximum standardized uptake value (SUVmax) and Hounsfield unit (HU) from single-photon emission computed tomography/computed tomography (SPECT/CT) and the signal intensity ratio (SIR) from magnetic resonance imaging (MRI).

This retrospective study included 64 patients (97 joints) who presented with TMJ pain and underwent both SPECT/CT and MRI between 2017 and 2023 at the Department of Oral and Maxillofacial Surgery, Gangnam Severance Hospital. Based on clinical and imaging criteria, joints were categorized into OA (65 joints) and normal (32 joints) groups. Quantitative comparisons were made between the groups for SUVmax, HU, and SIR values, and correlations among these parameters were analyzed.

The OA group showed a significantly higher SUVmax (median 6.5) than the normal group (median 3.1, $p < 0.0001$), indicating increased bone metabolic activity. HU values for both total condyle head and medulla were also higher in the OA group (719.0 and 394.0, respectively) compared to the normal group (552.2 and 290.5), suggesting enhanced bone sclerosis and formation. In contrast, SIR values were significantly lower in the OA group (0.9 on proton density weighted image (PDWI) and 1.03 on T2WI (T2 weighted image)) compared to the normal group (1.2 on PDWI and 1.16 on T2), indicating reduced perfusion or altered bone marrow composition.

MRI findings showed significant differences between the OA and normal groups about all parameters, including disc-condyle relationship, disc shape, bone marrow signal, joint space, and joint effusion. The OA group exhibited a higher prevalence of non-reducing disc displacement, deformed disc shapes, narrowed joint space, and decreased bone marrow signal, which are considered characteristic of TMJ OA.

Correlation analysis revealed a significant positive relationship between SUVmax and HU across all regions, and a significant negative correlation between SUVmax and SIR. Additionally, a negative correlation between SIR and HU was observed. These findings are interpreted as reflecting the pathophysiological progression of TMJ OA, where increased metabolic activity and bone density are accompanied by reduced vascular supply.

In conclusion, this study quantitatively analyzed various imaging parameters that reflect the pathophysiology of TMJ OA, suggesting their potential to overcome the limitations of conventional subjective or qualitative assessments in diagnosis and staging. SUVmax, HU, and SIR respectively reflect bone metabolism, density, and perfusion, and their integrated interpretation may serve as an effective tool for the quantitative diagnosis and prognostic evaluation of TMJ OA. Future large-scale studies considering age, sex, and disease progression stages are needed to enhance generalizability and establish clinical diagnostic criteria.

Key words : single-photon emission computed tomography/computed tomography, magnetic resonance imaging, maximum standardized uptake value, Hounsfield units, signal intensity ratio

1. INTRODUCTION

Temporomandibular joint osteoarthritis (TMJOA) is a gradual degenerative condition in the jaw joint, and affects 8–16% of the population worldwide, with an annual health expense of more than $80 billion. (Wang et al. 2023) Clinically, OA can be diagnosed both by symptoms found in a physical examination and through radiographic imaging. (Rando, Waldron 2012) The clinical symptoms of TMJOA are crepitus, jaw stiffness with pain, or progressively increasing anterior open bite. (Shi et al. 2017) The clinical diagnosis of TMJ OA needs to be validated through radiographic evaluation. The radiographic findings on patients with TMJ OA include subchondral bone sclerosis, erosion, osteophytes, flattening/irregularities or deformation of the condylar surface and reduction of joint space (Rando, Waldron 2012)

Various imaging methods are available for viewing the TMJ, including panoramic and transcranial radiographs, standard computed tomography (CT), corrected tomography, cone-beam CT (CBCT) and magnetic resonance imaging (MRI). (Brooks et al. 1997) Recently, Single-photon emission computed tomography/computed tomography (SPECT/CT) has been utilized to detect physiological changes in bone tissue, with maximum standardized uptake value (SUVmax) showing a strong correlation to conventional imaging markers of OA activity. (Kim et al. 2017, Ogura et al. 2020)

The CT has been the preferred technique for assessing the contours of the cortical bone

and TMJ dynamics. (dos Anjos Pontual et al. 2012) SPECT/CT is a hybrid imaging method that has emerged as a modern advancement in nuclear medicine for evaluating joint osteoarthritis. (Kim et al. 2017) By combining detailed CT imaging with SPECT, SPECT/CT allows precise anatomical localization of nuclear activity. It also yields measurable values such as SUV (maximum or mean) from SPECT and Hounsfield units(HU) from CT for evaluating bony or joint structures. (Cachovan et al. 2013) This combination allows for more precise detection of osseous abnormalities using nuclear imaging. (Kim et al. 2017) HU, a relatively quantitative measure of radio-density in CT, allows for a quantitative assessment of bone density during diagnosis and enables an objective evaluation of bone quality. (Zaidi, Danisa, Cheng 2019) SUV is used as a parameter for quantitative SPECT/CT imaging, representing the ratio of radioactivity concentration in a target voxel to the average radioactivity concentration in the body. (Toriihara et al. 2018)

MRI is widely utilized in diagnosing temporomandibular joint disorders (TMD) because it offers clear visualization of the disc, condyle, and glenoid fossa, as well as their spatial relationships, which facilitates accurate assessment of TMJ morphology. (Montesinos et al. 2019) Beyond structural changes in the mandibular condyle, its quality also influences disease prognosis. The blood supply to the condyle is crucial for growth, nutrient provision, and repair potential. Pathologic influence of the articular disc may reduce blood flow to the condyle, potentially leading to condylar resorption (Cai, Jin, Yang 2011) Therefore, condylar blood flow information can be valuable for assessing condylar state. In proton

density-weighted imaging (PDWI), magnetic signal intensity (MSI) can roughly reflect blood flow signals. (Wan et al. 2023) Wei et al. (Wei et al. 2002) reported that MSI has large individual variations, and thus used the signal intensity ratio (SIR) with MSI of the cerebral cortex as a reliable reference for standardizing. (Wei et al. 2002)

Huang et al. (Huang et al. 2015) insisted that the condyle's blood supply is essential for its growth, development, nutrient supply, and repair capacity. Elevated pressure may inhibit the development of both bone and blood vessels. Furthermore, it was observed that a reduction in blood supply could impair the synthesis of aminopolysaccharides in cartilage, contributing to osteoarthritis. (Ji, Resnick, Peacock 2020) However, SPECT/CT imaging has limitation that it is unable to assess blood flow. Moreover, there are no studies analyzing the condylar bone quantification and blood flow status in patients with TMJ OA.

In this retrospective study, we aim to raise a new method to quantitatively evaluate condylar quality by using the SIR on MRI and SUVmax and HU values on SPECT/CT to assist in the diagnosis of TMJ OA. We hypothesized that assessment of the condyle-to-cerebral cortex SIR on MRI as a noninvasive and quantitative method is useful in diagnosis and prognosis of TMJ OA. Specifically, we proposed three hypotheses: first, that HU would rise due to bone remodeling processes like osteosclerosis and osteophyte formation; second, that SUV would increase due to active bone metabolism; third, that SIR would decrease due to slow down blood flow.

2. PATIENTS AND METHODS

2.1. Participants

This retrospective study included patients presenting with TMJ-related pain or discomfort and who visited the Oral and Maxillofacial Surgery Department at Gangnam Severance Hospital, Yonsei University in Seoul, Korea, between January 2017 and September 2023. Following a clinical assessment, MRI and SPECT-CT examinations were performed within the same hospital, at the Department of Radiology and Nuclear Medicine. The diagnosis of OA was determined based on previously established criteria, including the DC/TMD diagnostic system and objective indicators, such as the presence of pain, a simultaneous hot spot on SPECT/CT, or bony changes such as sclerosis. In contrast, the normal group exhibited none of these features—no pain, no hot spot on SPECT/CT, and no bony changes.

Exclusion criteria for this study included: (1) an interval of more than six months between MRI and SPECT-CT examinations, (2) a prior history of radiation therapy to the head and neck area, (3) a confirmed diagnosis of rheumatoid arthritis, (4) a history of maxillofacial trauma or surgery involving the TMJ, and (5) patients with bony changes on MRI but without pain, or those experiencing pain in the masticatory muscles rather than in the TMJ itself.

In this study, patients were classified into the OA group if they presented with both a hot spot on SPECT/CT and clinical pain. Those without either a hot spot or clinical pain were classified into the normal group.

This study received approval from the Institutional Review Board of Gangnam Severance Hospital (Approval No. #3-2023-0320), with a waiver for written informed consent. All procedures adhered to the ethical principles outlined in the Declaration of Helsinki.

2.2. MRI evaluation

The assessment of disc morphology, relationship between the disc and condyle, bone marrow signal(BMS), fluid collection, and joint space was conducted through MRI, according to a prior study (Kim et al. 2018).

2.2.1. Relationship between the disc and condyle

The positional relationship between the disc and condyle was categorized into three distinct types: normal, anterior disc displacement with reduction, and anterior disc displacement without reduction (Kim et al. 2018) (Figure 1).

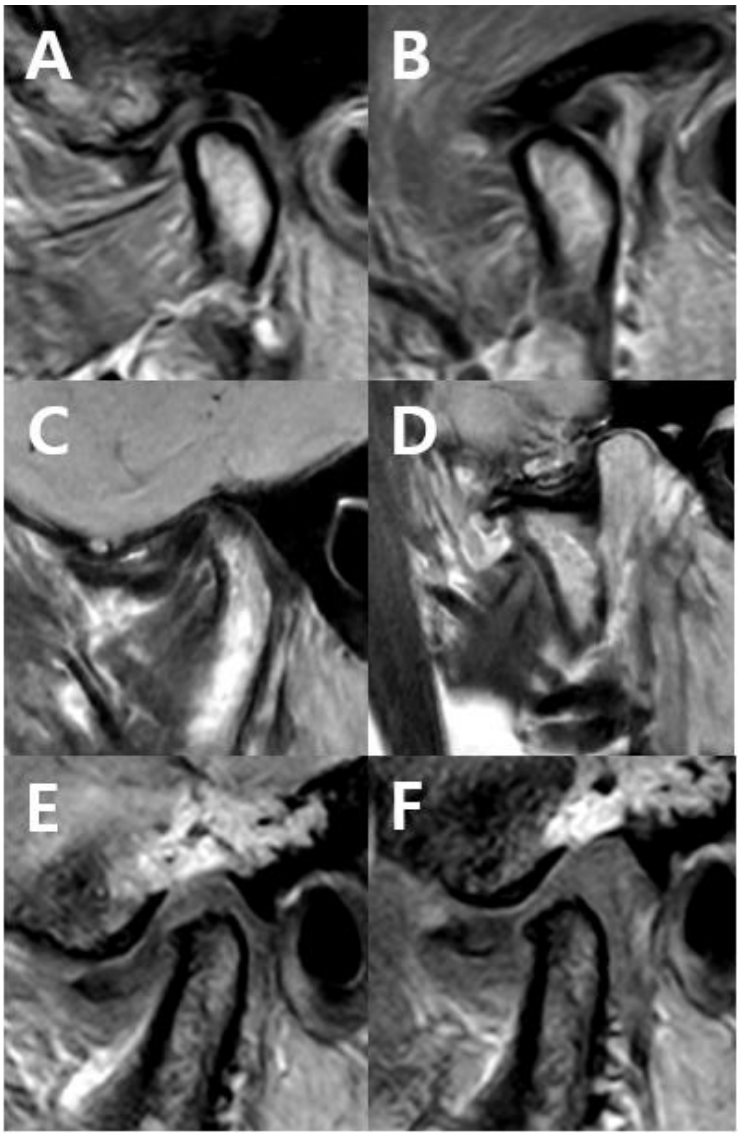

Figure 1. Relationship between condyle and disc. A, B, Normal disc position. C, D, anterior disc displacement with reduction (ADcR). E, F, anterior disc displacement without reduction (ADsR).

2.2.2. Disc shape

The morphology of the disc in closed-mouth MRI images was classified into five distinct categories: biconcave, folded, flattened, eyeglass, or amorphous (Figure 2). A biconcave disc was characterized by a normal structure and position within normal limits (WNL). Discs that seem like a cap or cup shape (∩- or ∪-shaped) without any shortened length on anterior band, intermediate area, and posterior band were categorized as folded. If the disc presented a biplanar shape with a reduction in volume in either the anterior or posterior band, or both, it was classified as flattened. Discs that displayed anteroposterior shortening were categorized as the eyeglass shape. Finally, discs with severe deformation, making their structure unidentifiable, were designated as amorphous. For cases where the disc demonstrated anterolateral or anteromedial displacement, and exhibited characteristics of more than two shape categories, the classification was determined by assigning the highest category (Huh, Kim, Ko 2003, Kim et al. 2018, Paesani et al. 1992).

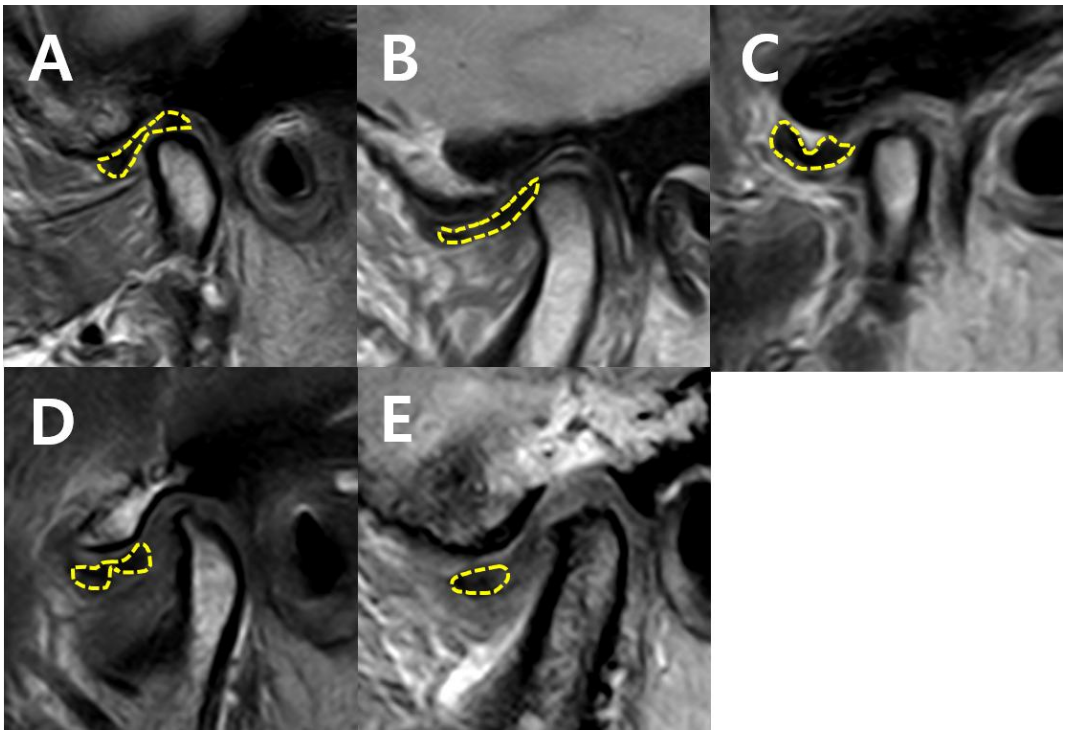

Figure 2. Disc shapes. Disc shapes were categorized into 5 types (dotted line). A, Biconcave. B, Flattened. C, Folded. D, Eyeglass-shaped. E, Amorphous

2.2.3. Bone marrow signal

Bone marrow signal (BMS) was categorized as either "WNL" or "low", based on its signal intensity on PDWI, in comparison to the ipsilateral ramus or mandibular body (Kim et al. 2018) (Figure 3).

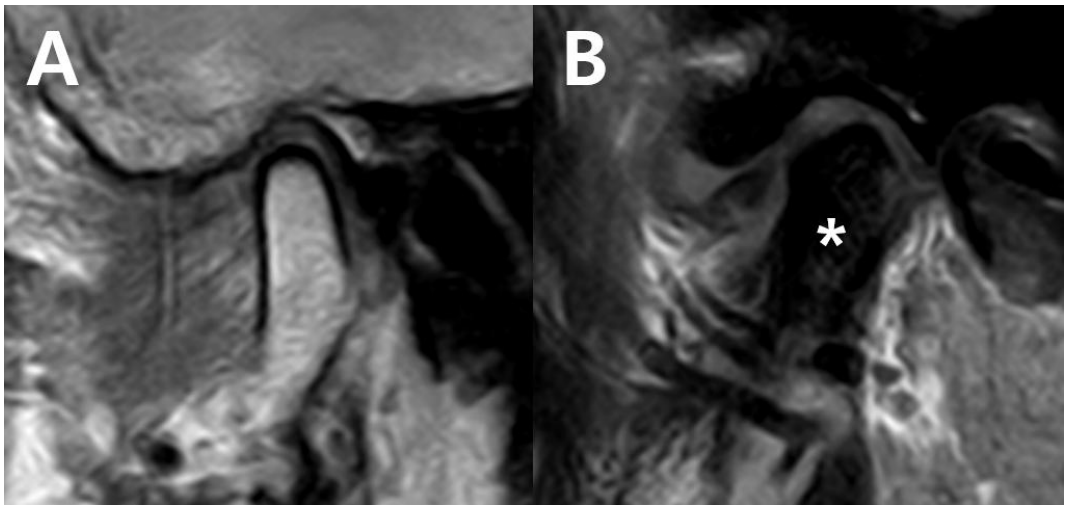

Figure 3. Bone marrow signal (BMS). The signal intensity of the condyle was evaluated in relation to that of the mandibular ramus or body. A, Normal BMS: similar signal intensity with ramus; B, low BMS: decreased signal intensity (asterisk).

2.2.4. Joint space

The joint space was categorized into three groups: “normal,” “narrowed,” and “bone-to-bone contact” (Figure 4). A narrowed joint space was defined as an insufficient gap between the condyle and fossa, preventing adequate accommodation of the disc. Bone-to-bone contact was characterized by no space between the cortical surfaces of the condyle and fossa, indicating either complete or nearly complete contact on closed-mouth images (Kim et al. 2018).

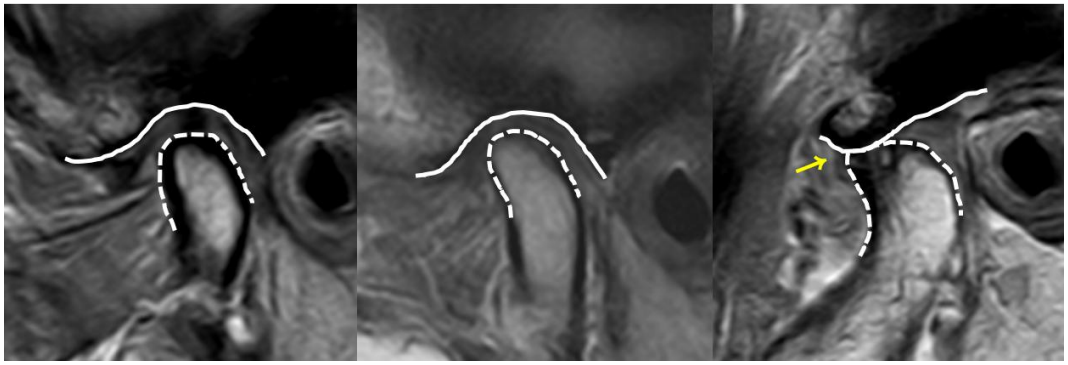

Figure 4. Joint space. Joint space was classified into three types based on the distance between the condyle (dotted line) and the fossa (solid line). A. Normal: sufficient space is present between the condyle and the condylar fossa. B. Narrowing: the space between the condyle and fossa is reduced. C. Bone-to-bone contact: the condyle and fossa are in direct contact with no intervening space (arrow).

2.2.5. Joint effusion

Joint effusion was assessed using T2WI. Following the criteria established in previous studies, it was classified into three categories based on the volume of fluid accumulation: G0, indicating either no detectable fluid or only a thin high-signal-intensity line; G1, where fluid was confined within the disc boundary; and G2, representing a moderate to large volume of fluid extending beyond the disc boundary or leading to capsular expansion (Huh, Kim, Ko 2003, Kim et al. 2018, Paesani et al. 1992) (Figure 5).

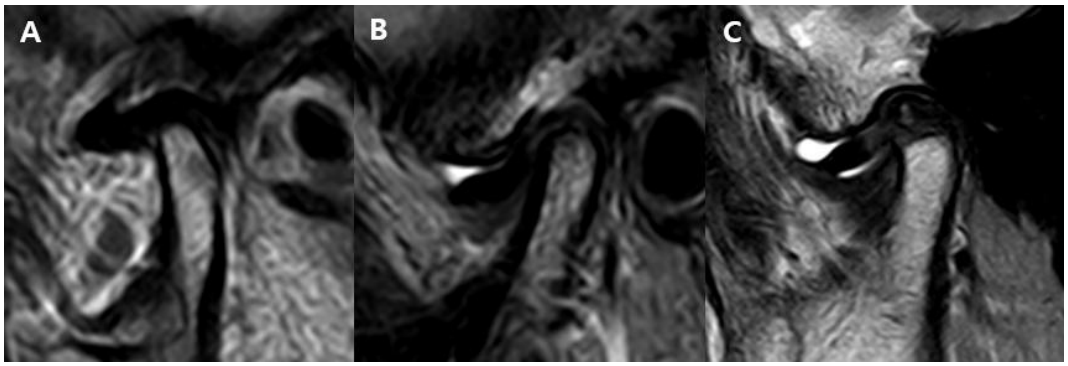

Figure 5. Fluid collection. A, G0: No fluid collection. B, G1: a small amount of fluid collection around disc boundary. C, G2: a large amount of fluid collection beyond disc boundary.

2.3. Measurement of SUV max

SPECT-CT imaging was conducted using the Symbia Intevo16 system (Siemens Healthineers, Erlangen, Germany). Scans were acquired from the top of the head to the lung apex three hours after intravenous administration of 740 MBq of 99mTc-hydroxydiphosphonate. The imaging parameters were set as follows: a rotation of 3° per step, an acquisition time of 20 seconds per projection, and a matrix size of 512 × 512. Low-dose CT images were obtained at 110 kV and 120 mA with adaptive dose modulation to optimize radiation exposure. Image reconstruction was performed by xSPECT Quant and xSPECT Bone software (Siemens Healthineers, Erlangen, Germany) to enhance resolution and ensure precise quantification.

Two nuclear medicine specialists (J.H. Lee and Y.H. Ryu) analyzed the images using the open-source software LIFEx (version 7.4.6; LIFEx, RRID:SCR_025284,

www.lifexsoft.org) (Nioche et al. 2018). A manually delineated spherical region of interest (ROI) was positioned at the center of the mandibular condyle and adjusted to include all relevant TMJ structures, referencing both coronal and axial CT images. The SUV was determined according to a previously established method, using the following formula:

$$\text{SUV max} = \frac{decay\text{-}corrected\ activity\ [kBq]\ per\ mL\ of\ tissue\ volume}{injected\ activity\ [kBq]\ per\ gram\ of\ body\ mass}$$

SUVmax was identified as the highest voxel intensity within the defined ROI.

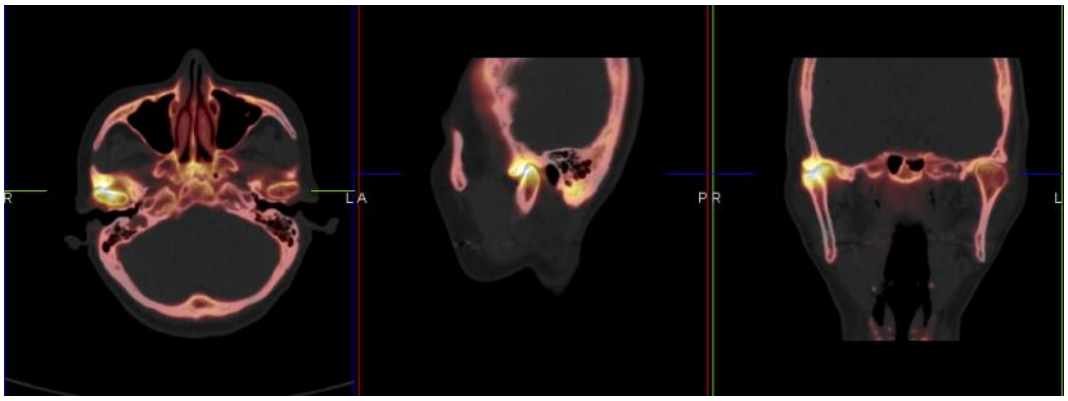

Figure 6. Hot spot indicating Increased bone uptake of condyle in bone scintigraphy

2.4. Measurement of HU

The HU of the mandibular condyle in SPECT/CT was assessed using the Centricity DICOM Viewer (GE Healthcare, Chicago, Illinois, USA). HU values were obtained using the ROI tool on the coronal plane, selecting the slice where the condyle appeared largest. The ROI, encompassing both cortical and medullary bone of condyle ("Cortical +

Medulla"), was defined from the uppermost point of the condyle to the condylar neck, identified as the narrowest section of the condylar process (Shi et al. 2017) (Figure 7).

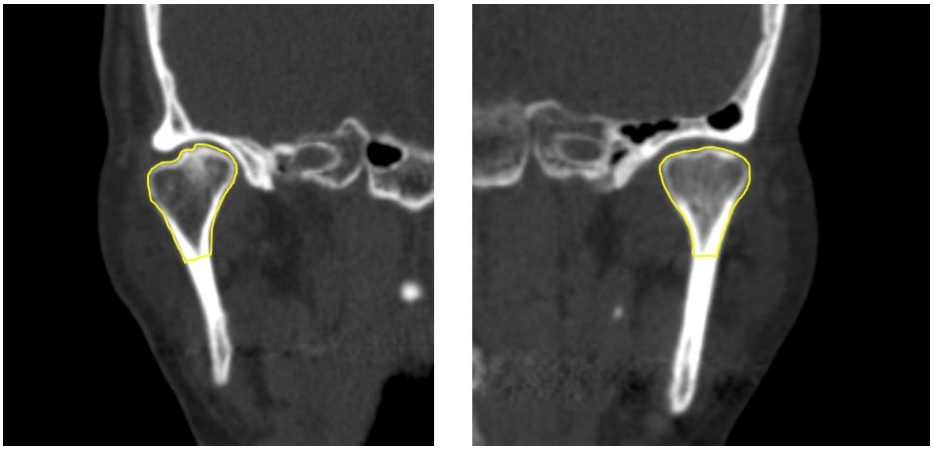

Figure 7. ROI of the condyle on coronal section of SPECT/CT

Additionally, HU measurements were separately recorded for the medullary ("Medulla") regions of both condyles (Figure 8). The Centricity DICOM Viewer automatically calculated the HU values.

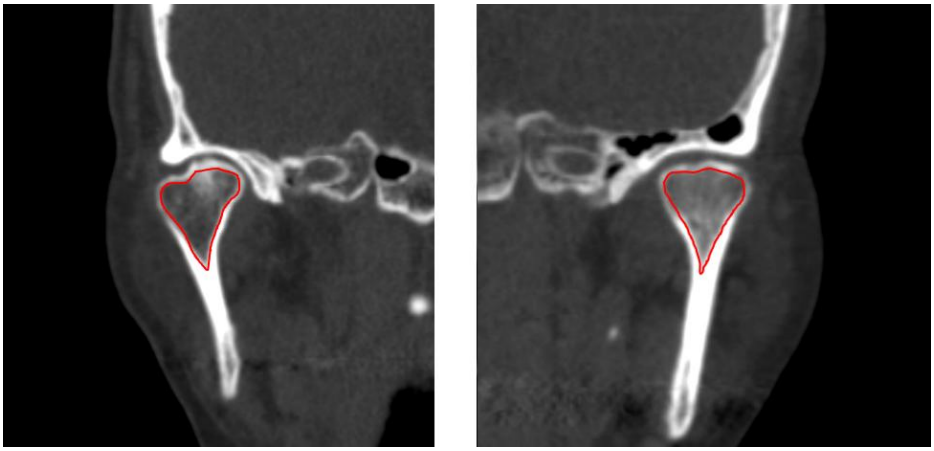

Figure 8. ROI of medullary (red line) bone of the condyle on coronal section of SPECT/CT

2.5. Measurement of SIR

MRI of the TMJ area was conducted using a 3.0-T Magnetom scanner (Achieva; Philips Medical Systems, Best, The Netherlands) equipped with 3-inch surface coils. The imaging protocol was identical to that used in a previous study (Kim et al. 2018). Specifically, PDWI was acquired with the following parameters: repetition time of 450 ms, echo time of 20 ms, slice thickness of 3 mm, field of view (FOV) of 120 mm, and an acquisition matrix size of 240 × 240. For T2 weighted imaging(T2WI), the parameters included a repetition time of 2900 ms and an echo time of 90 ms.

MRI imaging was analyzed using the Centricity DICOM Viewer (GE Healthcare, Chicago, Illinois, USA). Three images were selected from the middle third of the condyle on each side, corresponding to the largest cross-sectional area. MRI evaluation of the condyle was conducted at medullar bone of the condylar head, with the largest inscribed circle in slice.

For the cerebral cortex, MRI was conducted at the inferior temporal gyrus, aligning with the same plane of the condyle. Three measurements were taken from the inscribed circle within the same region on each side, and the mean value was recorded. The MSI was obtained for both the condyle (MSI1) and the cerebral cortex (MSI2), and the SIR was calculated as MSI1/MSI2 (Figure 9).

Edema in the bone marrow of the mandibular condyle has been considered a precursor to osteoarthritis and typically appears as high signal intensity on T2WI. Therefore, we

analyzed T2WI to assess bone marrow changes in patients with TMJ OA. (Schellhas et al. 1989) However, T2WI were not available for one patient, and thus this case was excluded from the SIR evaluation.

To ensure reliability in volume measurement, one observer (C.Lee, 4-year-experienced in oral and maxillofacial surgery) measured HU and SIR twice on one-third of the patients in minimum 4 weeks interval.

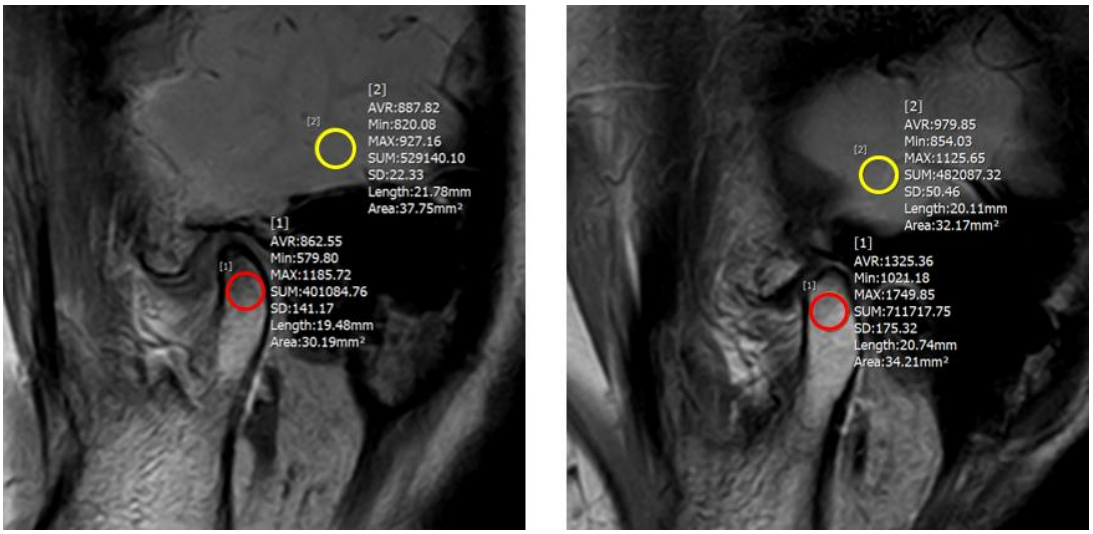

Figure 9. ROI of condyle (red circle) and cerebral cortex(yellow circle) on sagittal section of MRI PDWI

2.6. Statistical analysis

Statistical analyses were conducted using SPSS (version 27.0; SPSS Inc., Chicago, IL, USA) and SAS version 9.4 (SAS Institute, Cary, NC, USA). Intraclass correlation

coefficient (ICC) was evaluated. To determine differences between the Normal and OA groups, statistical tests were performed based on data type. For continuous variables, the Mann-Whitney U test was applied, while categorical variables were analyzed using the Chi-square test or Fisher's exact test, as appropriate. Spearman's rank correlation coefficient was conducted to examine the relationships among SIR, HU, and SUVmax within each of the Normal and OA groups, as well as within the overall sample. A p-value of less than 0.05 was considered statistically significant.

3. RESULTS

Totally, 64 patients (97 joints) were included in this study. Of these, 6 were male and 58 were female. Among 97 joints, the OA and normal groups included 65 joints (56 patients; 5 men and 51 women; age, 51.0, minimum 19.0 - maximum 80.0 years) and 32 joints (32 patients; 4 men and 28 women; age, 50.0, minimum 19.0 – maximum 81.0 years), respectively. 32 patients were diagnosed with OA on one side and normal TMJ on the other; therefore, they were included in both groups. Since the normality assumption was not met, a non-parametric Mann-Whitney U test was performed for statistical analysis. There was no significant difference in age ($p=0.8538$) and sex ($p=0.4717$) between the two groups. ICC for HU (total) 0.996 (0.986-0.999) in normal and 0.994 (0.985-0.997) OA groups. ICC for SIR on PDWI was 0.973 (0.903-0.993) in normal and 0.961(0.910-0.984) in OA groups. ICC for SIR on T2WI was 0.985 (0.944-0.996) in normal and 0.978(0.948-0.991) in OA groups. The results of demographic characteristics are summarized in Table 1.

Table 1. Clinical characteristics and Intraclass correlation coefficient (ICC) of the patients

	Normal	*OA*	*p-value*
No. of joints (patients)	32 (32)	65(56)	
Age† - median(min-max)	51.0 (19.0-80.0)	50.0 (19.0-81.0)	0.8538
Sex – n (%)*			0.4717
Male	4 (12.5)	5 (7.7)	
Female	28 (87.5)	60 (92.3)	
ICC (95% confident interval) ¶			
HU (Medulla)	0.998 (0.991-0.999)	0.995 (0.989-0.998)	
HU (total)	0.996 (0.986-0.999)	0.994 (0.985-0.997)	
SIR (PDWI)	0.973 (0.903-0.993)	0.961 (0.910-0.984)	
SIR (T2WI)	0.985 (0.944-0.996)	0.978 (0.948-0.991)	

OA, osteoarthritis; HU, Hounsfield Unit; SIR, signal intensity ratio; PDWI, proton density-weighted imaging; T2WI, T2 weighted image.

† Mann-Whitney U test was done.

* Chi-square test was done.

¶ ICC was calculated one-third of the joints. 11 and 22 joints were involved in normal and OA group, respectively.

3.1. Comparisons of MRI findings between normal and OA groups (Table 2)

A Chi-square test was conducted to compare the MRI findings between normal group and OA group. Statistically significant differences were observed between the two groups in all categories; Disc-Condyle relationship, Disc shape, Bone marrow signal, Joint Space, Joint

Effusion.

In Disc-Condyle relationship, the normal group had the highest frequency of normal cases, with 14 joints (43.8%). In contrast, in the OA group, the most common condition was anterior disc displacement without reduction (ADsR), observed in 54 joints (83.1%).

Regarding disc shape, in the normal group, the biconcave shape, which represents a normal disc shape, was the most frequently observed in 24 joints (75.0%), while the amorphous shape, the most deformed type, was not observed. Conversely, in the OA group, no joints had a biconcave shape, whereas the amorphous shape was the most frequently observed, accounting for 42 joints (64.6%).

For bone marrow signal, in the normal group, 31 joints (96.9%) exhibited signals within the normal range, with only one joint showing a weak signal. In contrast, in the OA group, 19 joints (29.2%) exhibited a weak signal.

Regarding joint space, in the normal group, the frequency distribution was as follows: Narrowing (19 joints; 59.4%), within normal limits (WNL) (13 joints; 40.6%), and bone-to-bone contact (0 joints; 0%), indicating that no case of bone-to-bone contact was observed. However, in the OA group, bone-to-bone contact was observed in 21 joints (32.3%). The distribution in the OA group was as follows: Narrowing (38 joints; 58.5%), bone-to-bone contact (21 joints; 32.3%), and WNL (6 joints; 9.2%).

For joint effusion, the G0 state, which indicates no detectable fluid or only a thin high-signal-intensity line, was observed in 78.1% (25 joints) of the normal group, occupying a

significant proportion. However, in the OA group, this proportion was less than half, at 41.5% (27 joints). Conversely, G1 and G2 states were observed at a higher rate in the OA group compared to the normal group. Specifically, in the normal group, G1 was found in 18.8% (6 joints) and G2 in 3.1% (1 joint), whereas in the OA group, G1 was observed in 36.9% (24 joints) and G2 in 21.6% (14 joints).

Table 2. Comparisons of MRI findings between normal and OA groups

	Normal	*Osteoarthritis*	*p-value*
Disc-Condyle relationship			<.0001
Normal	14 (43.8)	4 (6.1)	
ADcR	10 (31.2)	6 (10.8)	
ADsR	8 (25.0)	54 (83.1)	
Disc shape			<.0001
Biconcave	24(75.0)	0(0.0)	
Flattened	3(9.4)	8(12.3)	
Folded	4(12.5)	8(12.3)	
Sunglass	1(3.1)	7(10.8)	
Amorphous	0(0.0)	42(64.6)	
BMS			0.0028
WNL	31(96.9)	46(70.8)	
Low	1(3.1)	19(29.2)	
Joint Space			<.0001
WNL	13(40.6)	6(9.2)	

Narrowing	19(59.4)	38(58.5)	
Bone to Bone contact	0(0.0)	21(32.3)	
Joint Effusion			0.0021
G0	25(78.1)	27(41.5)	
G1	6(18.8)	24(36.9)	
G2	1(3.1)	14(21.6)	

ADcR, anterior displacement with reduction; ADsR, anterior displacement without reduction; BMS, bone marrow signal; WNL, within normal limits

Chi-square test was done.

3.2. Comparison of SUVmax, HU and SIR (Table 3)

To determine the differences between the Normal and OA groups, the Mann-Whitney U test was conducted for continuous variables, including SUVmax, HU (total and medulla) and SIR. The SUV max in the OA group was 6.5, which was higher compared to 3.1 in the normal group. For HU, in the medulla and the entire condyle head region, the OA group showed values of 394.0 and 719.0, respectively, which were higher than those observed in the normal group (290.5 and 552.2, respectively). On the other hand, SIR values were significantly lower in the OA group (0.9 on PDWI and 1.03 on T2WI) compared to the normal group (1.2 on PDWI and 1.16 on T2WI) All variables showed statistically significant differences between the Normal and OA groups.

Table 3. Comparison of SUVmax, HU (Total, Medulla), and SIR between the Normal and

OA Groups.

variables	total (n=97) Median (min-max)	Normal (n=32) Median (min-max)	OA (n=65) Median (min-max)	p-value
SUVmax	5.4 (2.1-23.5)*	3.1 (2.1-5.2)*	6.5 (2.1-23.5)*	<.0001
HU				
Medulla	351.0 (120.0-1203.0)*	290.5 (120.0-587.0)*	394.0 (123.0-1203.0)*	0.001
Total	683.3 (307.0-1330.0)*	552.2 (307.0-964.0)*	719.0 (437.0-1330.0)*	<.0001
SIR				
PDWI	1.0 (0.1-1.7)*	1.2 (0.8-1.7)*	0.9 (0.1-1.5)*	<.0001
T2WI	1.07 (0.13-1.76)*	1.16 (0.7-1.76)*	1.03 (0.13-1.38)*	0.003

OA, osteoarthritis; SUVmax, maximum standardized uptake value; HU, Hounsfield unit; SIR, signal intensity ratio; PDWI, proton density-weighted imaging; T2WI, T2 weighted image.

Mann-Whitney U test was done.

* $p < 0.05$

3.3. Relationships among SIR, HU (Total and Medulla), and SUVmax in the entire joints. (Table 4)

Spearman's rank correlation coefficient was conducted to examine the relationships among SIR, HU (Total and Medulla), and SUVmax. In the total sample, all correlations demonstrated statistical significance.

There was a positive correlation between SUVmax and HU in the medullary regions of the condyle, as well as in the total region of condyle head. In contrast, SUVmax showed a negative correlation with SIR. There was a negative correlation between SIR and HU in the medullary regions of the condyle, as well as in the total region of condyle head.

Table 4. Relationship among SUVmax, HU (Total and Medulla), and SIR in entire group.

Variables		SUVmax	HU		SIR
			Medulla	Total	
SUVmax	ρ	1.000	0.283*	0.322*	-.551*
	p-value	.	0.005	0.001	<0.001
SIR	ρ	-0.551*	-0.590*	-0.520*	1.000
	p-value	<0.001	0.006	<0.001	.

SUVmax, maximum standardized uptake value; HU, Hounsfield unit; SIR, signal intensity ratio; ρ, Spearman's rank correlation coefficient.

Spearman's rank correlation coefficient was done.

* $p < 0.05$

The following scatter plots visualize the findings described above.

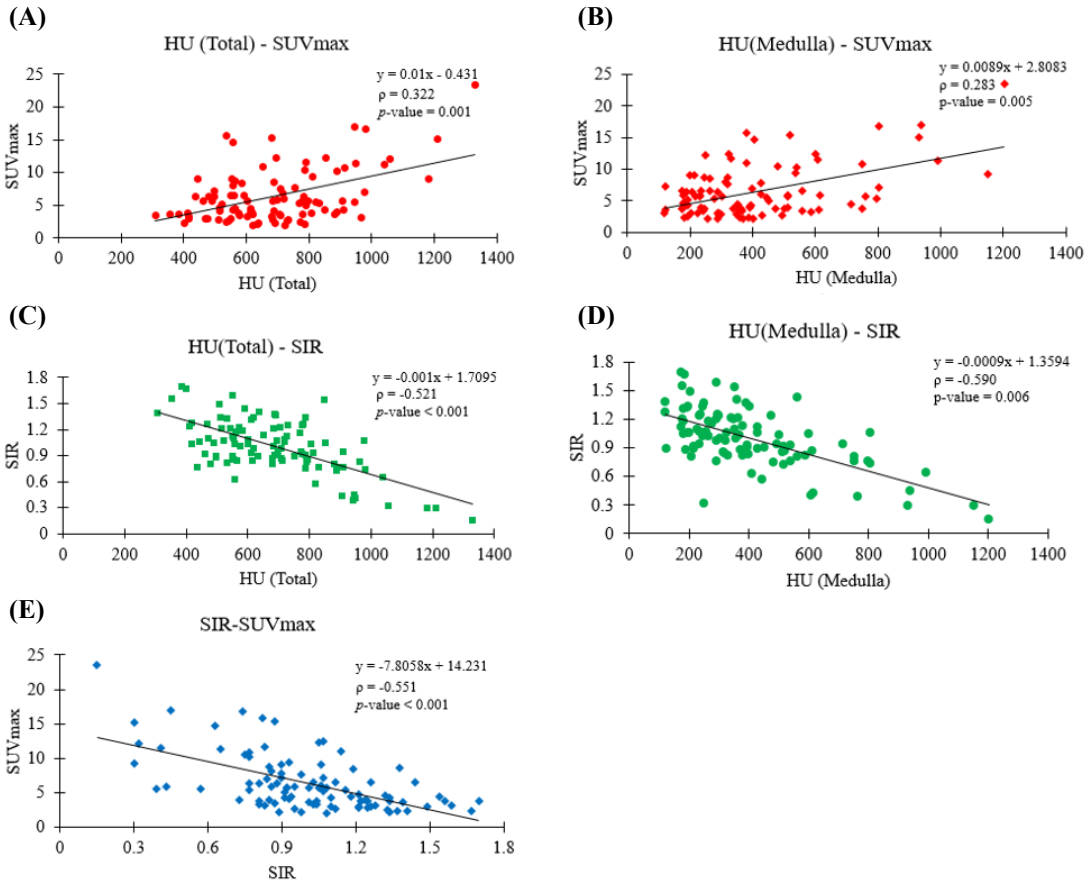

Figure 10. Correlation among SUVmax, HU (Total and medulla), and SIR in the entire subjects. (A) Correlation between HU (Total) and SUVmax; (B) Correlation between HU (Medulla) and SUVmax; (C) Correlation between HU (Total) and SIR; (D) Correlation between HU (Medulla) and SIR; (E) Correlation between SIR and SUVmax.

3.4. Relationships among SIR, HU (Total and Medulla), and SUVmax in the affected joints with OA. (Table 5)

To assess the relationships among SIR, HU (Total and Medulla), and SUVmax, Spearman's rank correlation coefficient was performed. The OA group exhibited a similar trend to that observed in the entire patient cohort.

An increase in SUVmax was correlated with higher HU values in the medulla and total condyle head regions. In contrast, as SUVmax increased, SIR showed a decreasing correlation. At this time, the correlation between SUVmax and HU was not statistically significant, whereas the correlation between SUVmax and SIR showed statistical significance. As SIR increased, the HU measured in the medulla, and total regions of the condyle head all showed a negative correlation, which was statistically significant.

Table 5. Relationship among SUVmax, HU (Total and Medulla), and SIR in OA group

Variables		**SUVmax**	**HU**		**SIR**
			Medulla	**Total**	
SUVmax	ρ	1.000	0.190	0.144	-0.373*
	p-value	.	0.129	0.252	0.002
SIR	ρ	-0.373*	-0.523*	-0.434*	1.000
	p-value	0.002	<0.001	<0.001	.

SUVmax, maximum standardized uptake value; HU, Hounsfield unit; SIR, signal intensity ratio; ρ, Spearman's rank correlation coefficient.

Spearman's rank correlation coefficient was done.

* $p < 0.05$

The following scatter plots visualize the findings described above.

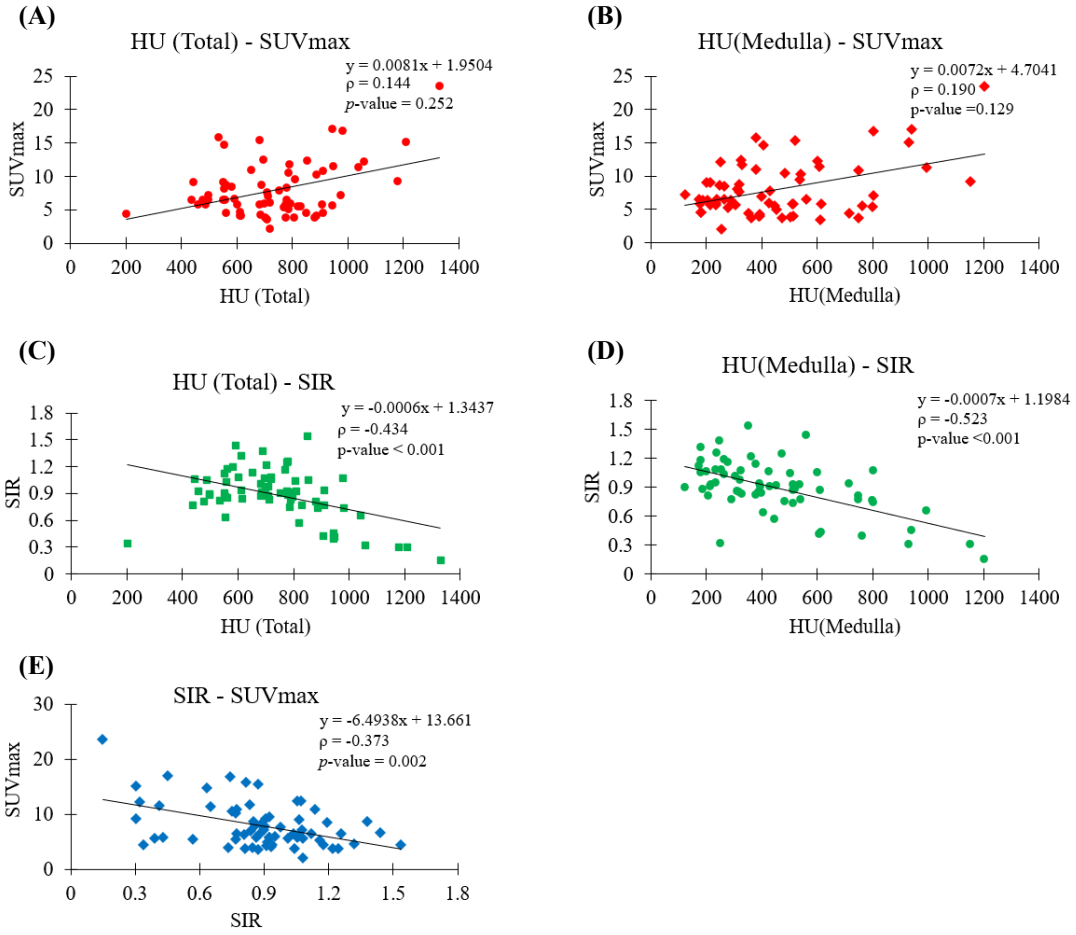

Figure 11. Correlation among SUVmax, HU (Total and medulla), and SIR in OA group. (A) Correlation between HU (Total) and SUVmax; (B) Correlation between HU (Medulla) and SUVmax; (C) Correlation between HU (Total) and SIR; (D) Correlation between HU (Medulla) and SIR; (E) Correlation between SIR and SUVmax.

3.5. Relationships among SIR, HU (Total and Medulla), and SUVmax in normal joints. (Table 6)

Spearman's rank correlation coefficient was utilized to evaluate the relationships among SUVmax, HU (Total and Medulla), and SIR. The HU values of the medulla and the entire condyle showed statistically significant correlations with both SIR and SUVmax, whereas the other combinations did not show statistical significance.

In the normal TMJ group, some findings differed from those described earlier. SUVmax showed a negative correlation with both HU and SIR. SIR, as previously described, also exhibited a negative correlation with HU.

Table 6. Relationship among SUVmax, HU (Total and Medulla), and SIR in normal group

Variables		SUVmax	HU		SIR
			Medulla	Total	
SUVmax	ρ	1.000	-0.370*	-0.440*	-0.009
	p-value	.	0.037	0.012	0.959
SIR	ρ	-0.009	-0.545*	-0.451*	1.000
	p-value	0.959	0.001	0.010	.

SUVmax, maximum standardized uptake value; HU, Hounsfield unit; SIR, signal intensity ratio; ρ, Spearman's rank correlation coefficient.

Spearman's rank correlation coefficient was done.

* $p < 0.05$

The following scatter plots visualize the findings described above

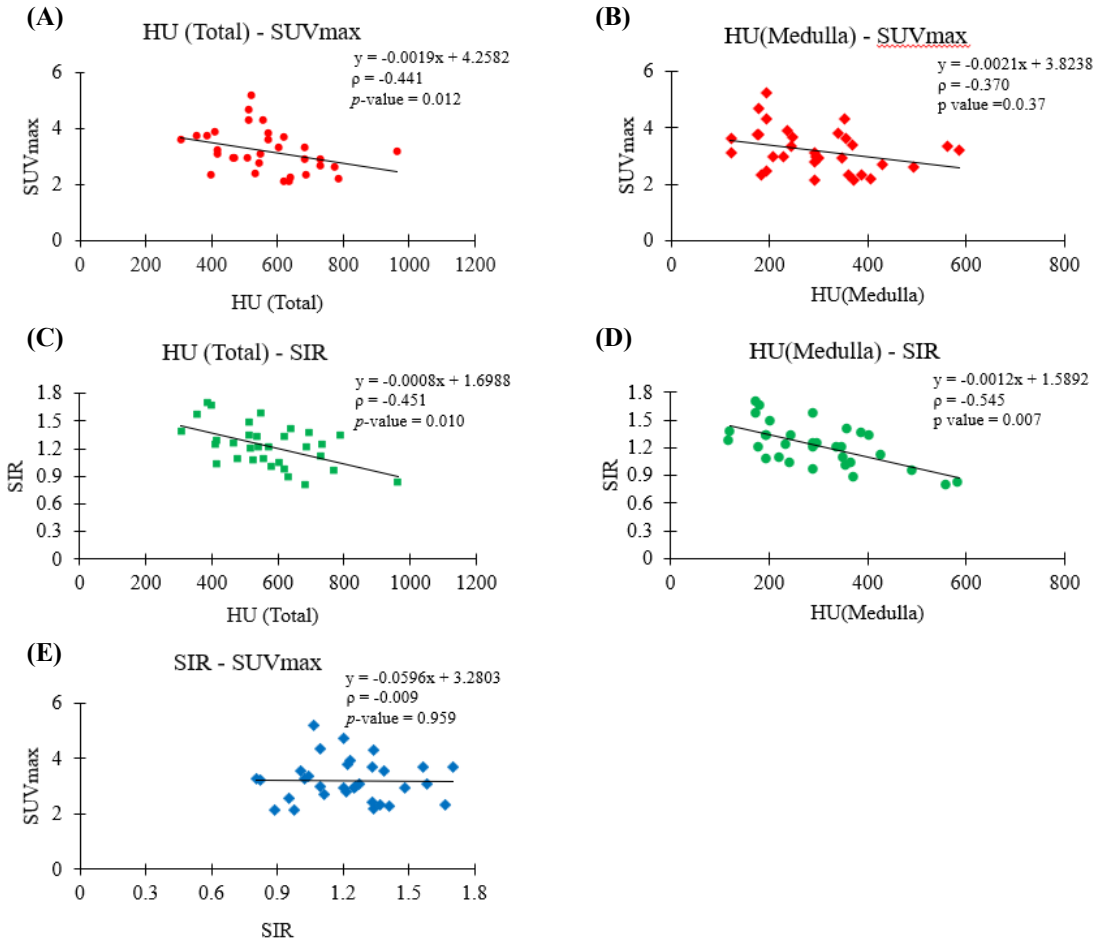

Figure 12. Correlation among SUVmax, HU (Total and medulla), and SIR in normal group

Correlation among SUVmax, HU (Total and medulla), and SIR in the entire subjects. (A) Correlation between HU (Total) and SUVmax; (B) Correlation between HU (Medulla) and SUVmax; (C) Correlation between HU (Total) and SIR; (D) Correlation between HU (Medulla) and SIR; (E) Correlation between SIR and SUVmax.

4. DISCUSSION

This retrospective study was for proposing quantitative evaluating methods of condylar quality by incorporating SIR from MRI and SUVmax and HU values from SPECT/CT, aiming to enhance the diagnostic process for TMJ OA. SPECT/CT and MRI can be used as quantitative tools to aid in diagnosing characteristic bone changes in TMJ OA, and numerous studies are conducted on this topic. (Kim et al. 2024, Wan et al. 2023) .

In clinical practice, there are several limitations in diagnosing TMJ osteoarthritis (OA). Pain is a highly subjective symptom, and its severity and characteristics can vary depending on the patient's perception, which reduces the objectivity of the diagnosis. Moreover, the origin of joint pain is not always related to bony changes or inflammation. For instance, pain may arise from surrounding soft tissues such as the lateral capsule or nearby ligaments, or it may be referred pain from masticatory muscles like the masseter or temporalis. These types of pain can easily be mistaken by patients as originating from the temporomandibular joint, leading to potential misdiagnosis of TMJ OA in clinical settings. In addition, radiographic evidence of bony changes does not necessarily correlate with pain symptoms and may not accurately reflect the disease activity or progression (Higuchi et al. 2020). Due to these limitations, recent studies have aimed to evaluate TMJ OA using more quantitative and objective methods.

According to a recent study by Kim et al., OA patients exhibit a higher average SUVmax on SPECT/CT compared to non-OA groups, with a cut off value of 5.15. They suggested that an SUVmax exceeding 5.15 indicates a high likelihood of OA (Kim et al. 2024). Shi et al. reported that assessing the HU value on CT can help diagnosing TMJ OA due to ability to evaluate the bone quality of the condyle (Shi et al. 2017). Additionally, a study by Wan et al. reported that in cases of condylar resorption, a typical feature of OA, the SIR value obtained from MRI(PDWI) tends to decrease. They further suggested that when the SIR falls below 0.78, condylar resorption is either already in progress or imminent, indicating the need for appropriate treatment (Wan et al. 2023).

The present study further supports these findings by demonstrating significant differences between OA and non-OA groups in terms of SUVmax, HU, and SIR values. Specifically, SUVmax was found to be significantly higher in the OA group (median 6.5, range 2.1–23.5) compared to the normal group (median 3.1, range 2.1–5.2). Similarly, HU values in the medulla and total condyle head were higher in OA patients than in normal subjects. On the other hand, on both PD-weighted and T2-weighted MRI, SIR values were significantly lower in the OA group than in the normal group, with measurements of 0.9 versus 1.2 on PDWI and 1.03 versus 1.16 on T2WI. It is consistent with previous studies suggesting that a decrease in SIR is associated with condylar resorption and the progression of TMJ OA.

Furthermore, correlation analysis revealed notable relationships among SUVmax, HU, and SIR. SUVmax and HU showed a positive correlation in the medulla, and total condyle head regions, indicating that higher bone metabolic activity (SUVmax) is associated with

increased bone density (HU). Conversely, SUVmax and SIR exhibited a negative correlation, suggesting that as bone metabolism increases, blood supply (represented by SIR) tends to decrease. Similarly, SIR and HU demonstrated a negative correlation, implying that as condylar resorption progresses, bone density declines.

All things considered in this study, these findings can be interpreted as reflective of the pathophysiological features of degenerative changes and bone remodeling associated with the progression of TMJ OA.

An increase in SUVmax indicates enhanced metabolic activity within the bone, suggesting that active bone remodeling is occurring in response to microdamage and inflammatory stimuli. This is consistent with previous reports demonstrating that osteoarthritic changes promote increased bone turnover as a compensatory mechanism to repair structural damage (Coutinho et al. 2006, Kim et al. 2024).

Similarly, the elevated HU values on CT correspond to bone sclerosis and increased mineral density. A study on knee osteoarthritis reported that subchondral sclerosis occurs in advanced osteoarthritic joints, and as mechanical loading increases, bone density rises compared to normal joints (Jaiprakash et al. 2012). Similar to the knee joint, the temporomandibular joint may also exhibit changes in bone patterns depending on the duration of the disease. In intermediate and late stages of OA, such adaptive responses often manifest as condyle sclerosis and osteophyte formation, which are radiographically observed as increased bone density (Jung 2023). While early-stage OA is often

characterized by reduced HU values as a result of bony resorption, the increased HU observed in the OA group in this study is presumed to reflect subchondral sclerosis associated with the intermediate to late stages of the disease. This suggests that the study cohort likely included a substantial number of patients in the intermediate to late stages of OA, in whom condylar sclerosis had already progressed.

Conversely, the observed decrease in SIR on both MRI PDWI and T2WI may indirectly reflect a reduction in vascular supply to the condyle or alterations in bone marrow composition. As TMJ OA progresses, narrowing of the joint space and the disc displacement may increase intra-articular pressure, subsequently compromising blood flow to the condyle. This vascular insufficiency can lead to bone marrow changes such as fibrosis or fatty infiltration, which are visualized on PDWI as reduced signal intensity. Therefore, decreased SIR may serve as an indirect marker of reduced physiological vitality of the condyle (Wan et al. 2023). Though T2WI is the most helpful in demonstrating the early changes of marrow congestion and inflammation, both of which increase marrow fluid and result in increased signal, the decreased SIR observed in our OA cohort may be attributed to late-stage remodeling and subchondral sclerosis, which corresponding signal loss on T2WI (Schellhas et al. 1989).

Taken together, the combination of increased SUVmax, elevated HU, and decreased SIR observed in this study represents a comprehensive imaging profile of TMJ OA pathophysiology. These findings encapsulate three key components of disease progression: increased metabolic activity, structural bone densification, and diminished vascularity and

tissue viability. The integration of these imaging parameters may offer valuable insights into TMJ OA activity and could contribute to a more accurate and objective assessment of TMJ OA in diagnosis.

This study has several limitations. First, as the primary objective was to investigate the imaging characteristics of SPECT-CT and MRI, the study did not consider the relationship between clinical symptoms, such as mouth opening limitation, and imaging findings. Second, the study did not consider when they start to be affected by TMJ OA. According to a previous study, an analysis of HU changes over time in TMJ OA revealed that HU values were lower in the early stage of TMJ OA, while they tended to increase in the intermediate and late stages. From a bone pattern perspective, the low HU in the early stage of TMJ OA can be attributed to degenerative changes such as bone erosion and resorption. In contrast, the increased HU in the intermediate and late stages may result from condylar remodeling due to inflammatory responses (Jung 2023). The patient population in this study tended to include more individuals in the intermediate and late stages of TMJ OA. Third, the study did not consider age and sex differences in SPECT-CT evaluations. Previous research has indicated that bone metabolic rates vary by age and sex, potentially leading to differences in imaging values (Kang et al. 2018). Since most patients in this study were female, the influence of sex-related differences is expected to be relatively minimal. However, further studies considering age differences are necessary to improve the accuracy of findings. Fourth, while this study aimed to clarify the patterns of SUVmax, HU, and SIR in TMJ OA patients, the different methods used to define the ROI for each

parameter may introduce variability, making the interpretation of correlations among these values somewhat controversial. Fifth, Bony changes were assessed using the CT images from SPECT/CT. However, this method has limitations in detecting subtle changes, which are more clearly visible on CBCT.

Despite these limitations, this study successfully identified the correlations among SUVmax, HU, and SIR in the diagnosis of TMJ OA. Future studies including a larger number of patients and incorporating additional factors may yield more precise and clinically significant results. These findings may ultimately contribute to the development of more accurate diagnostic protocols and individualized treatment strategies for TMJ OA.

5. CONCLUSION

This study confirms that SPECT/CT and MRI provide valuable quantitative metrics for diagnosing TMJ OA. The SUVmax, HU, and SIR values offer complementary insights into bone metabolism, density, and blood supply, respectively. The findings support the use of a combined imaging approach to improve the accuracy, objectivity, and reliability of TMJ OA diagnosis.

REFERENCES

Brooks, S. L., Brand, J. W., Gibbs, S. J., Hollender, L., Lurie, A. G., Omnell, K. A., Westesson, P. L., White, S. C. "Imaging of the temporomandibular joint: a position paper of the American Academy of Oral and Maxillofacial Radiology." *Oral Surg Oral Med Oral Pathol Oral Radiol Endod* 83, no. 5 (1997): 609-18. doi:10.1016/s1079-2104(97)90128-1.

Cachovan, M., Vija, A. H., Hornegger, J., Kuwert, T. "Quantification of 99mTc-DPD concentration in the lumbar spine with SPECT/CT." *EJNMMI Res* 3, no. 1 (2013): 45. doi:10.1186/2191-219X-3-45.

Cai, X. Y., Jin, J. M., Yang, C. "Changes in disc position, disc length, and condylar height in the temporomandibular joint with anterior disc displacement: a longitudinal retrospective magnetic resonance imaging study." *J Oral Maxillofac Surg* 69, no. 11 (2011): e340-6. doi:10.1016/j.joms.2011.02.038.

Coutinho, A., Fenyo-Pereira, M., Dib, L. L., Lima, E. N. "The role of SPECT/CT with 99mTc-MDP image fusion to diagnose temporomandibular dysfunction." *Oral Surg Oral Med Oral Pathol Oral Radiol Endod* 101, no. 2 (2006): 224-30. doi:10.1016/j.tripleo.2005.03.018.

dos Anjos Pontual, M. L., Freire, J. S., Barbosa, J. M., Frazao, M. A., dos Anjos Pontual, A. "Evaluation of bone changes in the temporomandibular joint using cone beam CT." *Dentomaxillofac Radiol* 41, no. 1 (2012): 24-9. doi:10.1259/dmfr/17815139.

Higuchi, K., Chiba, M., Sai, Y., Yamaguchi, Y., Nogami, S., Yamauchi, K., Takahashi, T. "Relationship between temporomandibular joint pain and magnetic resonance imaging findings in patients with temporomandibular joint disorders." *Int J Oral Maxillofac Surg* 49, no. 2 (2020): 230-6. doi:10.1016/j.ijom.2019.06.028.

Huang, L., Cai, X., Li, H., Xie, Q., Zhang, M., Yang, C. "The effects of static pressure on chondrogenic and osteogenic differentiation in condylar chondrocytes from temporomandibular joint." *Arch Oral Biol* 60, no. 4 (2015): 622-30. doi:10.1016/j.archoralbio.2015.01.003.

Huh, J. K., Kim, H. G., Ko, J. Y. "Magnetic resonance imaging of temporomandibular joint synovial fluid collection and disk morphology." *Oral Surg Oral Med Oral Pathol Oral Radiol Endod* 95, no. 6 (2003): 665-71. doi:10.1067/moe.2003.159.

Jaiprakash, A., Prasadam, I., Feng, J. Q., Liu, Y., Crawford, R., Xiao, Y. "Phenotypic characterization of osteoarthritic osteocytes from the sclerotic zones: a possible pathological role in subchondral bone sclerosis." *Int J Biol Sci* 8, no. 3 (2012): 406-17. doi:10.7150/ijbs.4221.

Ji, Y. D., Resnick, C. M., Peacock, Z. S. "Idiopathic condylar resorption: A systematic

review of etiology and management." *Oral Surg Oral Med Oral Pathol Oral Radiol* 130, no. 6 (2020): 632-9. doi:10.1016/j.oooo.2020.07.008.

Jung, Joon Ho. "Hounsfield Unit and Maximum Standardized Uptake Value of Temporomandibular Joint Osteoarthritis in SPECT/CT." *Graduate School, Yonsei University,* (2023).

Kang, J. H., An, Y. S., Park, S. H., Song, S. I. "Influences of age and sex on the validity of bone scintigraphy for the diagnosis of temporomandibular joint osteoarthritis." *Int J Oral Maxillofac Surg* 47, no. 11 (2018): 1445-52. doi:10.1016/j.ijom.2018.05.011.

Kim, J., Lee, H. H., Kang, Y., Kim, T. K., Lee, S. W., So, Y., Lee, W. W. "Maximum standardised uptake value of quantitative bone SPECT/CT in patients with medial compartment osteoarthritis of the knee." *Clin Radiol* 72, no. 7 (2017): 580-9. doi:10.1016/j.crad.2017.03.009.

Kim, J. Y., Jeon, K. J., Kim, M. G., Park, K. H., Huh, J. K. "A nomogram for classification of temporomandibular joint disk perforation based on magnetic resonance imaging." *Oral Surg Oral Med Oral Pathol Oral Radiol* 125, no. 6 (2018): 682-92. doi:10.1016/j.oooo.2018.02.009.

Kim, J. Y., Lee, C., Park, Y. L., Lee, J. H., Ryu, Y. H., Huh, J. K. "Diagnostic criteria for temporomandibular joint osteoarthritis using standardized uptake value in single-photon emission computed tomography-computed tomography." *Sci Rep* 14, no. 1 (2024): 31569. doi:10.1038/s41598-024-71639-1.

Montesinos, G. A., de Castro Lopes, S. L. P., Trivino, T., Sanchez, J. A., Maeda, F. A., de Freitas, C. F., Costa, A. L. F. "Subjective analysis of the application of enhancement filters on magnetic resonance imaging of the temporomandibular joint." *Oral Surg Oral Med Oral Pathol Oral Radiol* 127, no. 6 (2019): 552-9. doi:10.1016/j.oooo.2018.11.015.

Nioche, C., Orlhac, F., Boughdad, S., Reuze, S., Goya-Outi, J., Robert, C., Pellot-Barakat, C., Soussan, M., Frouin, F., Buvat, I. "LIFEx: A Freeware for Radiomic Feature Calculation in Multimodality Imaging to Accelerate Advances in the Characterization of Tumor Heterogeneity." *Cancer Res* 78, no. 16 (2018): 4786-9. doi:10.1158/0008-5472.CAN-18-0125.

Ogura, I., Sasaki, Y., Sue, M., Oda, T., Kameta, A., Hayama, K. "Tc-99m hydroxymethylene diphosphonate SPECT/CT for the evaluation of osteonecrosis of the jaw: preliminary study on diagnostic ability of maximum standardised uptake value." *Clin Radiol* 75, no. 1 (2020): 46-50. doi:10.1016/j.crad.2019.05.025.

Paesani, D., Westesson, P. L., Hatala, M. P., Tallents, R. H., Brooks, S. L. "Accuracy of clinical diagnosis for TMJ internal derangement and arthrosis." *Oral Surg Oral Med Oral Pathol* 73, no. 3 (1992): 360-3. doi:10.1016/0030-4220(92)90135-d.

Rando, C., Waldron, T. "TMJ osteoarthritis: a new approach to diagnosis." *Am J*

Phys Anthropol 148, no. 1 (2012): 45-53. doi:10.1002/ajpa.22039.

Schellhas, K. P., Wilkes, C. H., Fritts, H. M., Omlie, M. R., Lagrotteria, L. B. "MR of osteochondritis dissecans and avascular necrosis of the mandibular condyle." *AJR Am J Roentgenol* 152, no. 3 (1989): 551-60. doi:10.2214/ajr.152.3.551.

Shi, J., Lee, S., Pan, H. C., Mohammad, A., Lin, A., Guo, W., Chen, E., Ahn, A., Li, J., Ting, K., Kwak, J. H. "Association of Condylar Bone Quality with TMJ Osteoarthritis." *J Dent Res* 96, no. 8 (2017): 888-94. doi:10.1177/0022034517707515.

Toriihara, A., Daisaki, H., Yamaguchi, A., Kobayashi, M., Furukawa, S., Yoshida, K., Isogai, J., Tateishi, U. "Semiquantitative analysis using standardized uptake value in (123)I-FP-CIT SPECT/CT." *Clin Imaging* 52 (2018): 57-61. doi:10.1016/j.clinimag.2018.06.009.

Wan, S., Sun, Q., Xie, Q., Dong, M., Liu, Z., Yang, C. "The Retrospective Study of Magnetic Resonance Imaging Signal Intensity Ratio in the Quantitative Diagnosis of Temporomandibular Condylar Resorption in Young Female Patients." *J Pers Med* 13, no. 3 (2023). doi:10.3390/jpm13030378.

Wang, D., Qi, Y., Wang, Z., Guo, A., Xu, Y., Zhang, Y. "Recent Advances in Animal Models, Diagnosis, and Treatment of Temporomandibular Joint Osteoarthritis." *Tissue Eng Part B Rev* 29, no. 1 (2023): 62-77. doi:10.1089/ten.TEB.2022.0065.

Wei, X., Warfield, S. K., Zou, K. H., Wu, Y., Li, X., Guimond, A., Mugler, J. P., 3rd, Benson, R. R., Wolfson, L., Weiner, H. L., Guttmann, C. R. "Quantitative analysis of MRI signal abnormalities of brain white matter with high reproducibility and accuracy." *J Magn Reson Imaging* 15, no. 2 (2002): 203-9. doi:10.1002/jmri.10053.

Zaidi, Q., Danisa, O. A., Cheng, W. "Measurement Techniques and Utility of Hounsfield Unit Values for Assessment of Bone Quality Prior to Spinal Instrumentation: A Review of Current Literature." *Spine (Phila Pa 1976)* 44, no. 4 (2019): E239-E44. doi:10.1097/BRS.0000000000002813.

국문요약

단일 광자 방출 컴퓨터 전산화 단층촬영 및 자기공명영상을 이용한 측두하악관절 골관절염 환자의 하악과두 골 변화에 대한 정량적 평가

< 지도교수 김 재 영 >

연세대학교 대학원 치의학과
이채연

측두하악관절 골관절염은 관절 연골의 퇴행성 변화와 그에 따른 골의 재형성 및 기능 저하를 동반하는 만성 질환으로, 임상적으로는 저작 시 통증, 개구 제한, 관절 잡음 등의 증상으로 나타난다. 그러나 이러한 증상들은 주관적이며 다양한 원인에 의해 유사한 증상이 발생할 수 있어, 정확한 진단을 위해 영상학적 평가가 필수적이다.

기존의 방사선 영상에서는 골의 형태적 변화만을 평가할 수 있었으나, 최근에는 기능적 영상기법의 발전을 통해 골의 대사활성이나 혈류 상태를 반영한 정량적 분석이 가능해지고 있다. 이에 본 연구에서는 단일 광자 방출 컴퓨터 전산화 단층촬영에서 측정 가능한 최대 표준 흡수 계수율과 하운스필드 단위, 그리고 자기공명영상에서의 신호강도비를 활용하여 턱관절 골관절염 환자에서 하악과의 골 대사, 골밀도, 혈류 상태를 종합적으로 평가하고자 하였다.

본 연구는 2017 년부터 2023 년까지 강남세브란스병원 구강악안면외과에 내원한 TMJ 통증 환자 중 단일 광자 방출 컴퓨터 전산화 단층촬영 및 자기공명영상을 모두 촬영한 64 명의 환자(97 개의 턱관절)를 대상으로 수행된 후향적 연구이다. 환자는 영상 및 임상 기준에 따라 골관절염군(65 개 관절)과 정상군(32 개 관절)으로 분류되었다. 각 군 간 최대 표준 흡수 계수율, 하운스필드 단위 및 신호강도비의 정량적 지표 차이를 비교하고, 이들 간의 상관관계를 분석하였다.

분석 결과, 골관절염군은 최대 표준 흡수 계수율의 중앙값이 6.5 로, 정상군의 3.1 보다 유의하게 높았으며($p<0.0001$), 이는 골관절염에서의 골 대사활성 증가를 반영하는 소견으로 해석된다. 하운스필드 단위 역시 골관절염군에서 과두 전체에서의 하운스필드 단위(719.0) 및 골수 하운스필드 단위(394.0)가 정상군(552.2 및 290.5)에 비해 높아, 골경화 및 골형성 증가를 시사하였다. 반면,

자기공명영상에서 측정된 신호강도비는 골관절염군(PDWI 0.9, T2WI 1.03)에서 정상군(PDWI 1.2, T2WI 1.16)보다 유의하게 낮았으며(PDWI $p<0.0001$, T2WI $p=0.003$), 이는 골수의 혈류 감소나 구성 변화로 인한 신호강도 저하를 시사한다.

자기공명영상의 평가에서도 관절원판-하악과두 사이의 관계, 관절원판 형태, 골수 신호, 관절 공간, 관절 삼출액의 모든 항목에서 골관절염군과 정상군 간 유의한 차이가 확인되었다. 특히 골관절염군은 비정복성 관절원판변위와 변형된 관절원판 형태, 좁은 관절공간, 감소한 골수 신호에 대한 평가가 정상군에 비해 현저히 많았으며, 이러한 소견들은 골관절염의 상태와 밀접한 관련이 있는 것으로 여겨진다.

정량 지표들 간의 상관분석 결과, 최대 표준 흡수 계수율과 하운스필드 단위는 모든 영역에서 유의한 양의 상관관계를 보였으며, 최대 표준 흡수 계수율과 신호강도비는 유의한 음의 상관관계를 나타냈다. 신호강도비와 하운스필드 단위 간에도 음의 상관관계가 확인되었는데, 이는 골의 대사활성 증가 및 밀도 증가와 동시에 혈류가 감소하는 병태생리적 과정을 반영한 결과로 해석된다.

결론적으로, 본 연구는 측두하악 골관절염의 병태생리를 반영하는 다양한 영상학적 지표들을 정량적으로 통합 분석함으로써, 질환의 정확한 진단과 상태 평가에 있어 기존의 주관적 또는 정성적 평가의 한계를 보완할 수 있는 가능성을

제시하였다. 최대 표준 흡수 계수율은 골 대사 상태, 하운스필드 단위는 골질, 신호강도비는 혈류 상태를 각각 반영하는 지표로서, 이들 세 가지 지표의 종합적 해석은 측두하악 골관절염의 정량적 진단 및 예후 평가에 있어 효과적인 도구가 될 수 있다.

향후 보다 다양한 연령대와 성별, 질병 진행 단계를 고려한 대규모 연구를 통해 본 연구 결과의 일반화 가능성을 높이고, 임상 적용을 위한 진단 기준의 확립으로 이어질 수 있을 것이다.

핵심되는 말 : 단일 광자 방출 컴퓨터 전산화 단층촬영, 자기공명영상, 하운스필드 단위, 표준 흡수 계수율, 신호강도비, 턱관절, 골관절염